Real-time detection of airborne asbestos by light scattering from magnetically re-aligned fibers

Christopher Stopford, Paul H. Kaye,* Richard S. Greenaway, Edwin Hirst, Zbigniew Ulanowski, and Warren R. Stanley

Centre for Atmospheric and Instrumentation Research, University of Hertfordshire, Hatfield, Hertfordshire AL10 9AB, UK

**p.h.kaye@herts.ac.uk*

Abstract: Inadvertent inhalation of asbestos fibers and the subsequent development of incurable cancers is a leading cause of work-related deaths worldwide. Currently, there is no real-time in situ method for detecting airborne asbestos. We describe an optical method that seeks to address this deficiency. It is based on the use of laser light scattering patterns to determine the change in angular alignment of individual airborne fibers under the influence of an applied magnetic field. Detection sensitivity estimates are given for both crocidolite (blue) and chrysotile (white) asbestos. The method has been developed with the aim of providing a low-cost warning device to tradespeople and others at risk from inadvertent exposure to airborne asbestos.

OCIS codes: (120.4640) Optical instruments; (120.5820) Scattering measurements; (290.5850) Scattering, particles.

References and links

1. Testimony of NIOSH on occupational exposure to asbestos, tremolite, anthrophyllite and actinolite. 29CFR, Parts 1910 and 1926. 9 May, 1990.
2. World Health Organization, Factsheet Number 343 – July 2010. *http://www.who.int/mediacentre/factsheets/fs343/en/index.html*
3. P. Lilienfeld, P. B. Elterman, and P. Baron, "Development of a prototype fibrous aerosol monitor," Am. Ind. Hyg. Assoc. J. **40**(4), 270–282 (1979).
4. A. P. Rood, E. J. Walker, and D. Moore, "Construction of a portable fiber monitor measuring the differential light scattering from aligned fibers," Aerosol Sci. Technol. **17**(1), 1–8 (1992).
5. E. Kauffer, P. Martin, M. Grzebyk, M. Villa, and J. C. Vigneron, "Comparison of two direct-reading instruments (FM-7400 and Fibrecheck FC-2) with phase contrast optical microscopy to measure the airborne fibre number concentration," Ann. Occup. Hyg. **47**(5), 413–426 (2003).
6. C. F. Bohren and D. R. Huffman, *Absorption and Scattering of Light by Small Particles* (Wiley,1983), Chap. 8.
7. E. Hirst and P. H. Kaye, "Experimental and theoretical light scattering profiles from spherical and non-spherical particles," J. Geophys. Res-Atmos. **101**(D14), 19231–19235 (1996).
8. P. H. Kaye, "Spatial light scattering as a means of characterizing and classifying non-spherical particles," Meas. Sci. Technol. **9**(2), 141–149 (1998).
9. K. B. Aptowicz, R. G. Pinnick, S. C. Hill, Y. L. Pan, and R. K. Chang, "Optical scattering patterns from single urban aerosol particles at Adelphi, Maryland, USA: A classification relating to particle morphologies," J. Geophys. Res. **111**(D12), D12212 (2006).
10. P. H. Kaye, K. Aptowitz, R. K. Chang, V. Foot, and G. Videen, "Angularly resolved elastic scattering from airborne particles," in *Optics of Biological Particles*, A. Hoekstra, V. Maltsev, G. Videen, eds., 31–61 (Springer, 2007).
11. R. Cotton, S. Osborne, Z. Ulanowski, E. Hirst, P. H. Kaye, and R. S. Greenaway, "The ability of the Small Ice Detector (SID-2) to characterize cloud particle and aerosol morphologies obtained during flights of the FAAM BAe-146 research aircraft," J. Atmos. Ocean. Technol. **27**(2), 290–303 (2010).
12. E. Hirst, P. H. Kaye, and J. A. Hoskins, "Potential for recognition of airborne asbestos fibres from spatial light scattering profiles," Ann. Occup. Hyg. **35**(5), 623–632 (1995).
13. P. Kaye, E. Hirst, and Z. Wang-Thomas, "Neural-network-based spatial light-scattering instrument for hazardous airborne fiber detection," Appl. Opt. **36**(24), 6149–6156 (1997).
14. V. Timbrell, "Alignment of respirable asbestos fibres by magnetic fields," Ann. Occup. Hyg. **18**(4), 299–311 (1975).

#185720 - $15.00 USD Received 20 Feb 2013; revised 9 Apr 2013; accepted 15 Apr 2013; published 2 May 2013

15. P. Lilienfeld, “Method and apparatus for real time asbestos aerosol monitoring,” US patent 4,940,327. Filed Oct. 25 (1988).
16. Z. Ulanowski and P. H. Kaye, “Magnetic Anisotropy of Asbestos Fibers,” Appl. Phys. (Berl.) **85**(8), 4104–4109 (1999).
17. V. Prodi, T. De Zaiacomo, D. Hochrainer, and K. Spurny, “Fibre collection and measurement with the inertial spectrometer,” J. Aerosol Sci. **13**(1), 49–58 (1982).
18. L. Jianzhong, Z. Weifeng, and Y. Zhaosheng, “Numerical research on the orientation distribution of fibers immersed in laminar and turbulent pipe flows,” J. Aerosol Sci. **35**(1), 63–82 (2004).
19. R. E. Walpole and R. H. Myers, *Probability and Statistics for Engineers and Scientists, 5th edition* (Macmillan, 1993) Chap.10.

1. Introduction

Inadvertent inhalation of carcinogenic asbestos fibers disturbed by demolition or maintenance work has become a leading cause of work related deaths throughout the industrialized world. In 1990, the US National Institute for Occupational Safety and Health (NIOSH) stated that there is “no evidence for a threshold or 'safe' level of asbestos exposure” [1], a view supported since by the ever-decreasing statutory limits of exposure in industrialized countries. In 2010, the World Health Organization estimated that ~100,000 people die each year from asbestos-related lung cancer, mesothelioma and asbestosis resulting from occupational exposure [2].

Asbestos is found in five ‘amphibole’ forms, characterized by needle-like straight fibers (see Fig. 1), the most common being crocidolite (blue) and amosite (brown), and a ‘serpentine’ form, chrysotile (white), characterized by curved fibers. Generally, the amphiboles are regarded as even more carcinogenic than the more abundant chrysotile.

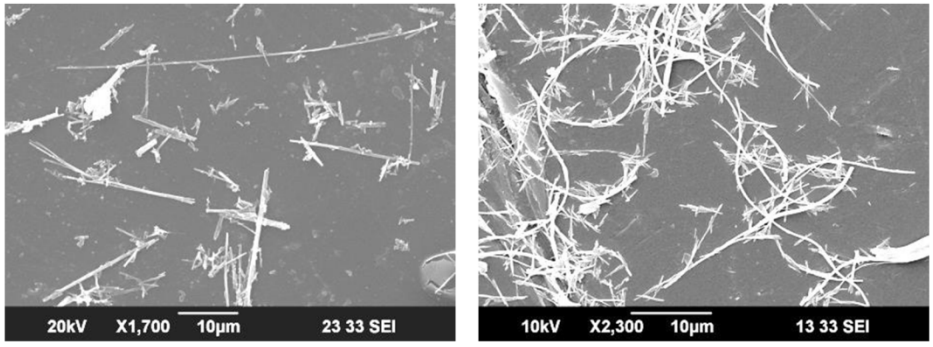

Fig. 1. Scanning electron micrographs of crocidolite (blue) and chrysotile (white) asbestos. Samples were respirable reference materials from UICC (International Union Against Cancer).

The most commonly used method for assessing airborne asbestos fiber concentrations is based on filter cassette sampling of the ambient air. Filters are subsequently removed for examination by phase contrast light microscopy (PCM) to count fibers having predefined length and minimum aspect ratio (typically 5 µm to 15 µm and 3:1 respectively) within grid areas. This process can determine fiber concentration in the sampled air but cannot establish whether the fibers are asbestos or a less hazardous material such as, for example, mineral wool, glass, or gypsum, a common fibrous material widely used in building fabrics. To achieve unambiguous asbestos identification, the detected fibers must undergo crystallographic analysis by energy dispersive x-ray technology (EDAX). These counting and analysis procedures are laborious and expensive to perform, and perhaps most importantly, provide results only many hours after the sampling (and possible inadvertent exposure of personnel) has occurred. Several attempts have therefore been made to address methods by which real-time in situ detection of airborne asbestos may be achieved.

An example is the comparatively widely used M7400AD Real-time Fiber Monitor (MSP Corp., Shoreview, MN) originally developed by Lilienfeld et al. [3]. This elegant instrument draws particle-laden air through a laser scattering chamber that is enveloped by a quadruple

#185720 - $15.00 USD Received 20 Feb 2013; revised 9 Apr 2013; accepted 15 Apr 2013; published 2 May 2013

electrode arrangement. It achieves fiber detection by aligning the fibers in an oscillating electric field, illuminating the fibers with the beam from a laser, and detecting the resulting oscillatory scattered light with a photomultiplier. The characteristic frequency, phase and shape of the pulses enable discrimination between the fibers of interest and other non-fibrous particles. Rood et al. [4], described a low-cost portable fiber monitor based on the differential light scattering produced by fibrous particles deposited electrostatically in uniform alignment onto a glass substrate. The device was capable of detecting airborne fibers but was not designed to detect individual particles, relying instead on the summation of scattering signals from a multitude of deposited fibers in order to achieve a detectable signal.

The Fibrecheck FC-2 (SMH Products Ltd., U.K.) is another light scattering instrument designed to detect fibrous particles in an ambient airflow. Again, discrimination between fibrous and non-fibrous particles is achieved by using several discrete detectors to measure differences in azimuthal scattering of laser light by individual particles. The performance of the Fibrecheck and FM7400 (a precursor to the M7400) instruments were compared by Kauffer et al. [5].

While these instruments are valuable tools for determining the presence of airborne fibers (and most fibers carry some inhalation risk) none are capable of discriminating between asbestos and non-asbestos fibers. Indeed, to date, there has been no unambiguous method for the detection of airborne asbestos fibers in real-time. This research therefore sought to provide such a capability. Importantly, our objective was not to emulate the statutory filter-based and EDAX protocols for assessing maximum permitted 'post-clearance' levels of airborne asbestos exposure (typically 0.1 fibers ml^{-1} in a 400 litre sample), but instead sought to provide a method of rapidly detecting airborne asbestos with high statistical confidence (99%) in a normal work environment. Specifically, we hope to provide tradespeople such as plumbers, electricians and builders, who might disturb asbestos while drilling walls or abrading pipes, with a low-cost monitor to warn against inadvertent asbestos exposure.

2. Methodology

Our approach is based on analysis of spatial light scattering patterns from individual airborne particles carried in an airstream sampled from the local environment. The analysis seeks to establish firstly whether each particle is a fiber or not, and if so, to then determine the extent to which the fiber has been re-aligned in a prevailing magnetic field. This latter measurement exploits the unique paramagnetic properties of asbestos minerals to allow their differentiation from other non-asbestos fiber types.

2.1 Spatial light scattering

The manner in which a particle scatters light is a complex function of the particle's size, shape and orientation, as well as properties (such as polarization and wavelength) of the illuminating radiation [6]. Consequently, when a particle is illuminated by a light source, such as a laser beam, the resulting complex pattern of scattered light can in many cases be used to classify the particle's morphology and orientation. Figure 2 illustrates a schematic optical arrangement for capturing scattering patterns from individual airborne particles and the widely varying patterns that can result.

Spatial light scattering analysis, also in certain geometries referred to as Two-dimensional Angular Optical Scattering (TAOS), has therefore attracted considerable attention for particle characterization in environmental, occupational and meteorological fields (see for example [7–11],) where a rapid assessment of the morphology of an airborne particle can lead to particle classification and in some cases particle identification.

#185720 - $15.00 USD Received 20 Feb 2013; revised 9 Apr 2013; accepted 15 Apr 2013; published 2 May 2013

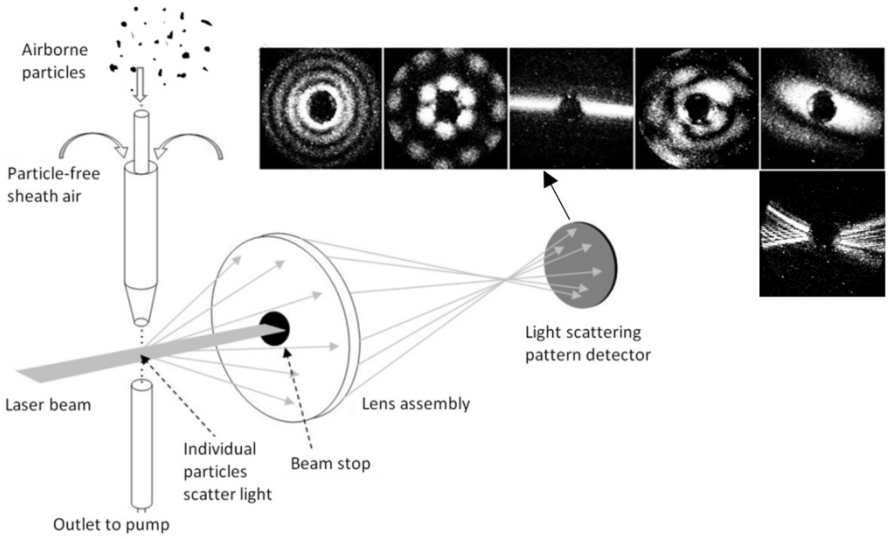

Fig. 2. Schematic illustration of spatial light scattering pattern acquisition from individual airborne particles. The example images shown were captured from particles using an intensified CCD camera as a detector. (Top row L-R): a ~9 μm water droplet, a cubic NaCl crystal (~4 μm), a straight crocidolite asbestos fiber, a cornflour grain, a 3 μm hematite ellipsoid. (Second row): a curved chrysotile asbestos fiber.

In the 1990's, the authors investigated the use of spatial light scattering for the identification of hazardous airborne fibers [12]. Detailed 2D images of scattering patterns from individual particles (similar to those in Fig. 2) showed that the straight needle-like fibers of crocidolite asbestos produced well-defined linear scattering orthogonal to the fiber axis. In contrast, the slightly curved fibers of chrysotile asbestos resulted in divergent or 'bow-tie' patterns (as in Fig. 2), with longer fibers producing greater divergence [12].

In our attempt to produce a real-time fiber detector, the intensified CCD camera used to capture the type of images shown in Fig. 2 was replaced by a custom-designed circular photodiode array comprising 32 azimuthal wedge-shaped elements [13]. This detector resulted in scattering pattern data of far lower spatial resolution than achieved with the CCD camera but allowed capture of single particle data 50 times faster. The distinctive linear scattering pattern from fiber particles allowed their efficient detection within a population of non-fibrous particles, but again, the technique could not differentiate between highly dangerous asbestos fibers and far less hazardous but generally more common fibers of, for example, glass, gypsum, or mineral wool that might have similar morphology.

2.2 Magnetic alignment of asbestos fibers

Almost uniquely among fibrous materials, asbestos has a magnetic susceptibility that results in a magnetic torque when the material is in the presence of a magnetic field. Timbrell [14] studied this effect in 1975 and showed that liquid-borne fibers of asbestos would align parallel or perpendicular to an applied magnetic field. Lilienfeld [15] filed a patent in 1988 that described a method for asbestos detection that employed an oscillating electric field to align and oscillate fibrous particles carried within a sample flow and a subsequent oscillating electromagnetic field to differentiate asbestos fibers. No further publication on this approach has been found, suggesting that the method was perhaps not pursued for technical reasons.

Ulanowski [16] found that the alignment of asbestos fibers in a magnetic field was due to the anisotropy of paramagnetic susceptibility within the fibers. He measured the magnitude of the magnetic torque on a fiber within a magnetic field by placing a small (70 μl) circular vessel containing asbestos fibers suspended in an isopycnic liquid at the center of a rotating

#185720 - $15.00 USD Received 20 Feb 2013; revised 9 Apr 2013; accepted 15 Apr 2013; published 2 May 2013

turntable. When a magnetic field was placed across the dish, it was possible to balance the forces due to magnetism with those due to viscous drag. He found that the torque on a fiber was proportional to sin 2θ, where θ was the angle between the fiber axis and the field. It followed that the maximum torque was experienced when the fiber was at 45° to the field.

He went on to use these results to predict the time it would take a similar asbestos fiber suspended in air to change alignment through a measurable angle, arbitrarily chosen to be 10°. The results, given in Fig. 3, showed that when exposed to a 0.5 T magnetic field at 45° to the fiber axis, airborne crocidolite and chrysotile asbestos fibers could be expected to re-align through a 10° angle in mean times of 0.14 ms and 1.8 ms respectively, depending on fiber size and aspect ratio.

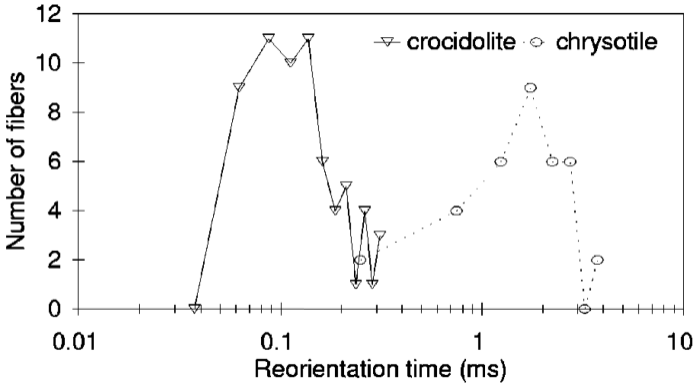

Fig. 3. Distribution of calculated times for airborne asbestos fibers to rotate through 10° in the presence of a 0.5T magnetic field initially at 45° to the fibers. [Reproduced from J. App. Phys. 84, 8, 4104-4109 (1999)].

This meant that if the change of angle of an individual fiber in a magnetic field could be measured accurately and rapidly, the potential existed of using the approach to help the real-time discrimination of airborne asbestos fibers from other fiber types. This paper describes such a development. Initially, a single laser beam apparatus was developed in which the change in orientation angle of fibers pre-aligned by a laminar flow delivery system was measured. Subsequently, a dual-beam method was developed that offered significantly greater accuracy and improved asbestos detection sensitivity.

3. Single-beam system

The Single-beam system was developed using Zemax optical design software (Radiant Zemax Inc., Redmond, WA) and is shown schematically in Fig. 4. The beam from a 30 mW 658 nm diode laser module (Prophotonix Inc., Salem, NH) is focused to an elliptical cross-section, approximately 3 mm wide and 0.1 mm deep at the intersection with a sample airflow carrying suspended particles from the ambient environment. The intersection of the beam with the airflow defines the so-called 'sensing volume'. The probability of more than one particle being present in this volume at any instant is small (<1%) even for high particle concentrations up to ~10^4 ml^{-1}. This ensures that predominantly single-particle light scattering data are recorded by the apparatus.

Particle-laden air is drawn by an air-sampling pump through a 50 mm long 1.5 mm bore stainless-steel delivery tube at a velocity of 4 ms^{-1} ± 0.5 ms^{-1}. The resulting flow in the tube is laminar with a parabolic flow-profile that has the effect of preferentially aligning elongated particles, such as fibers, towards the axis of the flow [17,18]. Set immediately above the intersection of beam and airflow are two high-strength N48 neodymium magnets (6 mm diameter, 13 mm length), arranged such that the field between them is at 45° to the axis of the airflow.

#185720 - $15.00 USD Received 20 Feb 2013; revised 9 Apr 2013; accepted 15 Apr 2013; published 2 May 2013

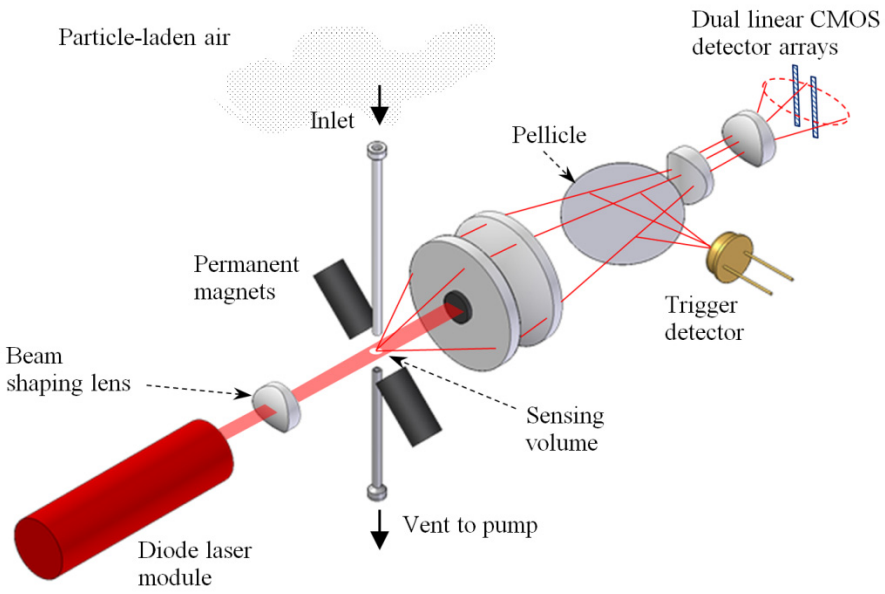

Fig. 4. Schematic diagram of the Single-beam scattering system used to (a) differentiate fibers from non-fiber particles in the sample air and then (b) to measure the angle of orientation of the fiber particles relative to the airflow axis. The latter parameter can be used to indicate whether or not the fibers had been rotated during transit through the magnetic field, thereby indicating if they were asbestos. For clarity, the enclosure containing this optical assembly is not shown.

Light scattered by individual particles passing through the laser beam is collected over forward scattering angles (5° to 20° to the beam axis) by the optical assembly, with the main laser beam being absorbed by a beam-dump as shown. About 8% of the collected scattered light is then reflected by a pellicle beam-splitter (a microscope cover-slip) onto a photodiode 'trigger' detector. The amplified signal from this detector is used both to assess particle size and to initiate the subsequent particle scattering pattern acquisition process.

The transmitted portion of the scattered light passes through two cylindrical lenses before falling onto two linear 512 pixel CMOS arrays (Hamamatsu Corp., model S9227) arranged vertically, 4.2 mm either side of the system optical axis. The sole purpose of these cylindrical lenses is to vertically compress the scattering pattern image and hence increase the range of azimuthal scattering angles covered by each CMOS array, as illustrated in Fig. 4.

3.1 Discriminating fibers from all other particles

Figure 5 below shows three examples of experimental CMOS array data recorded from individual airborne particles using the Single-beam apparatus. The particles were a crocidolite fiber (left), a water droplet approximately 11µm diameter (center), and an irregular shaped silica dust grain. In each case, the vertical axis covers the 512 array pixels and the horizontal axes either side of the centerline show the relative scattered light intensity recorded by each array (shown in red and green for clarity). The inset images are for illustration only and show the relative positions of the arrays (red and green bars) superimposed on typical scattering patterns (previously recorded using an intensified CCD camera) from these particle types.

#185720 - $15.00 USD Received 20 Feb 2013; revised 9 Apr 2013; accepted 15 Apr 2013; published 2 May 2013

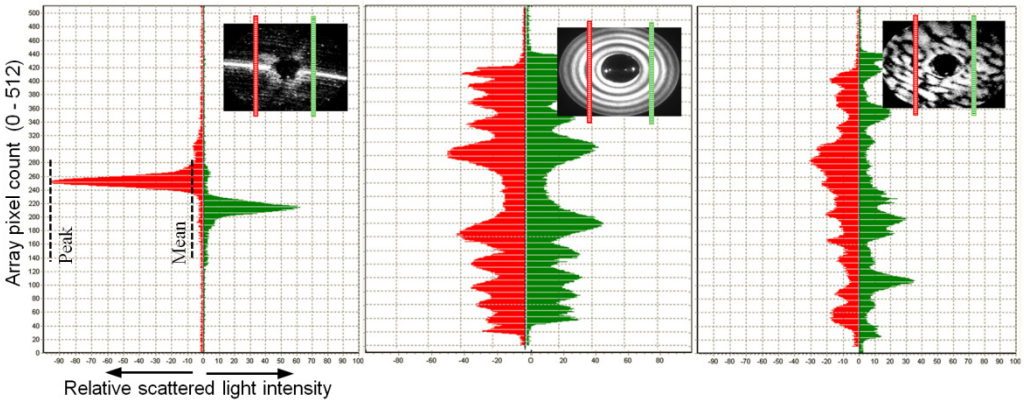

Fig. 5. CMOS linear array scattering data from a crocidolite fiber (left), a droplet (center), and an irregular shaped silica dust grain (right). The inset images are for illustration only and show the relative positions of the arrays (red and green bars) superimposed on the type of scattering patterns that would produce the given array responses. (Note the slight vertical offset of the 'green' array data. This is due to a small (~0.25 mm) misalignment of the two array chips on their printed circuit board and is corrected for in subsequent data processing).

The distinctive linear scattering from a fiber, exhibiting a dominant single peak in each array, provides a powerful means of discriminating fibers from other non-fibrous particles. Furthermore, the relative positions of the peaks can be used to determine the orientation angle of the fiber in the plane orthogonal to the laser beam, a critical requirement for our asbestos detection strategy. Note that if the fiber is also tilted out of this plane, the transfer properties of the lens system used to capture the scattered light results in both peaks exhibiting the same small vertical offset. Since it is the relative positions of the peaks that are of importance (see below), such 'global' offsets are of little consequence.

In contrast to fiber scattering, a spherical droplet passing through the laser beam (center example in Fig. 5) produces a scattering pattern comprising concentric rings; the outputs of the CMOS linear arrays intersecting these rings reflect this symmetry. Similarly, an irregular shaped dust particle (right) produces array outputs that have no distinctive peaks or symmetry.

A fast and computationally efficient method of discriminating between fiber and non-fiber particles has been implemented by simply evaluating the ratio of the peak intensity value in each array to the mean intensity of all pixels in that array ('Peak-to-Mean' ratio, or PTM). In the examples given in Fig. 5, the PTM values were 11.1, 2.2, and 3.4 for the fiber, droplet, and dust grain respectively.

Figure 6 gives an example of the distribution of PTM values recorded from airborne particles in a building environment where renovation work, involving plasterboard partition and ceiling tile removal, was being undertaken. Asbestos was known not to be present. Also shown in Fig. 6 are the PTM values recorded from laboratory generated aerosols of crocidolite and chrysotile asbestos (the materials shown in Fig. 1).

The results show that the airborne dust at the renovation location produced PTM values predominantly less than about 10. Approximately 2% of particles had higher PTM values indicating the presence of some airborne fibers, possibly of gypsum or synthetic fabric. The chrysotile asbestos produced a distribution with approximately 40% having PTM values greater than 10 (i.e. regarded as fibers) but still some 60% with PTM less than 10, despite being a fibrous material. This result was explained by microscopy of filter-captured particles which confirmed the tendency of the curved chrysotile fibers to clump. Such fiber aggregates would be regarded as 'non-fibers' by the PTM test, just as they would in a statutory phase-contrast microscopy analysis of filter-captured asbestos. More than 70% of the crocidolite

#185720 - $15.00 USD Received 20 Feb 2013; revised 9 Apr 2013; accepted 15 Apr 2013; published 2 May 2013

asbestos produced PTM values greater than 10, reflecting this material's tendency to produce pristine straight fibers that are less prone to clumping and aggregation.

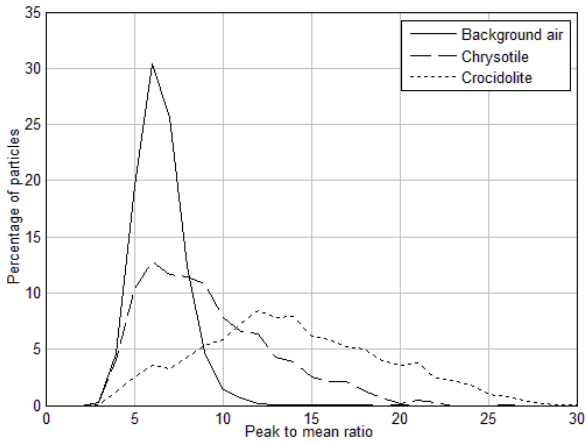

Fig. 6. Example of Peak-to-Mean (PTM) ratios for airborne particles found background air in an asbestos-free building renovation site (solid line), contrasted with PTM ratios recorded from laboratory aerosols of chrysotile (dashed line) and crocidolite (dotted line) asbestos. (Approximately 3,000 particles are represented in each distribution).

Based on the above, our results to date have employed a Peak-to-Mean threshold of 10 to discriminate between fiber and no-fiber particles (the latter including fiber aggregates).

3.2 Discriminating asbestos fibers from all other fibers

Once a pristine fiber has been identified using the PTM test, further processing of the array data allows estimation of the angle of alignment of that fiber to the airflow axis (within the plane perpendicular to the laser beam) at the moment it passed through the beam. This angle is determined from the geometry of the projected scattering pattern image onto the two CMOS arrays, as illustrated schematically in Fig. 7.

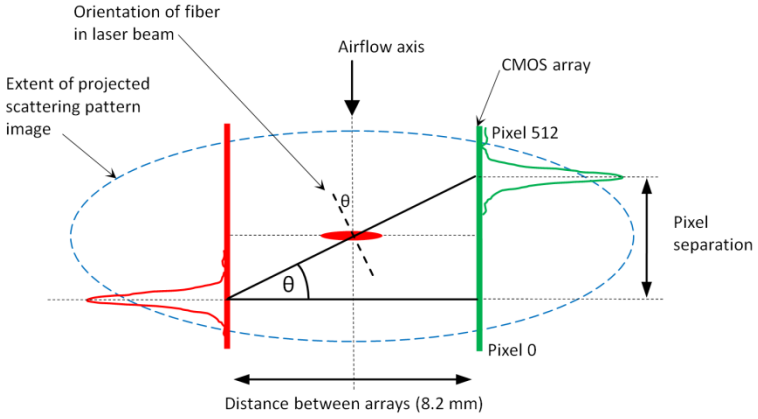

Fig. 7. Estimation of the fiber alignment angle (θ) of the fiber in the laser beam (beam cross-section shown as red ellipse) by measuring the separation of scattering peaks on the two CMOS arrays. The fiber itself is orthogonal to the line linking the scattering peaks, as indicated.

The angle θ is determined from a knowledge of the CMOS array separation (8.2 mm), the scatter peak separation (measured in pixels, where the pixel pitch is 0.0125 mm), and the

#185720 - $15.00 USD Received 20 Feb 2013; revised 9 Apr 2013; accepted 15 Apr 2013; published 2 May 2013

vertical compression of the scattering image (x3) resulting from the cylindrical lens in front of the arrays. Both fiber discrimination and fiber alignment angle can be determined in the prototype Single-beam system for particle throughputs approaching 600 particles/s.

Figure 8 shows experimental laboratory results recorded from an aerosol of crocidolite asbestos fibers both with and without the influence of the magnetic field. The red line in Fig. 8 shows the distribution of fiber alignment angles for more than 2,000 fibers with no magnetic field present. The parabolic flow profile in the delivery tube results in over 86% of fibers lying at an angle less than ± 10° to the airflow axis, although the range of angles naturally adopted by the fibers in the flow extended to about ± 30°. The blue line shows the fiber angle distribution for a similar number of fibers of the same asbestos material but with the magnets present. The distribution has been moved through approximately 7° to the right (corresponding to a re-alignment of the fibers towards the magnetic field direction). This re-alignment compares well with predicted values based on the airflow velocity at the laser beam (4 ms^{-1} +/– 0.5 ms^{-1}) and the measured magnetic flux density between the magnets of 0.26 T.

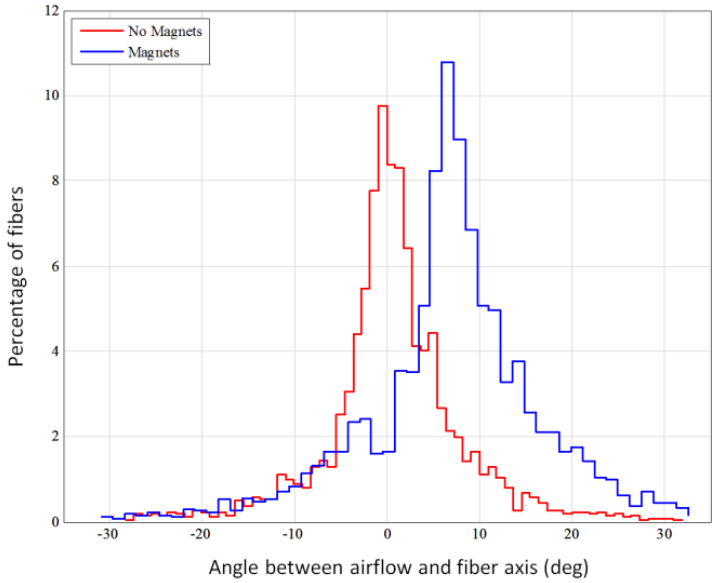

Fig. 8. Distribution of the alignment angle (relative to the airflow axis) of crocidolite fibers both with (blue) and without (red) a magnetic field present. (2,380 and 2,393 fibers are represented in the blue and red plots, respectively).

Results such as those in Fig. 8 were repeated for different aerosols of both asbestos and non-asbestos fibers. These confirmed that if a fiber was detected with an alignment angle of greater than + 20°, the probability of the fiber being asbestos was approximately 6 times higher than the probability it being a non-asbestos fiber that, by chance, had attained that angle of alignment. This meant that in a 'real-world' measurement situation such as a demolition site, if the concentration of non-asbestos fibers was comparable to or lower than that of the asbestos fibers, positive detection of the asbestos could be achieved with relatively few individual fiber measurements (see below). However, if the concentration of non-asbestos fibers exceeded that of asbestos fibers, the confidence with which a fiber measured at >20° alignment could be deemed 'asbestos' would be reduced accordingly, leading to an undesirable risk of false-positive asbestos detection.

4. Dual-beam system

The performance of the Single-beam system was fundamentally limited because the initial alignment of each fiber before it entered the magnetic field, although distributed around the

#185720 - $15.00 USD Received 20 Feb 2013; revised 9 Apr 2013; accepted 15 Apr 2013; published 2 May 2013

airflow axis, (red curve in Fig. 8) was not accurately known. What was required, therefore, was precise knowledge of both the initial alignment of the fiber before it entered the magnetic field and the final alignment on exiting the field. The Dual-beam system shown in Fig. 9 implements these measurements and allows the absolute change in fiber alignment to be measured for each individual fiber passing through the system.

In the Dual-beam system, two laser beams are arranged symmetrically above and below the optical axis, separated by a distance of 3 mm. The sample airflow column between the beams is permeated by the magnetic field at 45° to the airflow axis in the plane perpendicular to the laser beams. (This angle was later changed, as described below). The beam separation is a compromise between (a) the desire to retain a single optical detection system with acceptably low aberrations, and (b) the need for fibers carried in the sample airflow to be exposed to the magnetic field for sufficient time to induce measurable re-alignment of asbestos fibers.

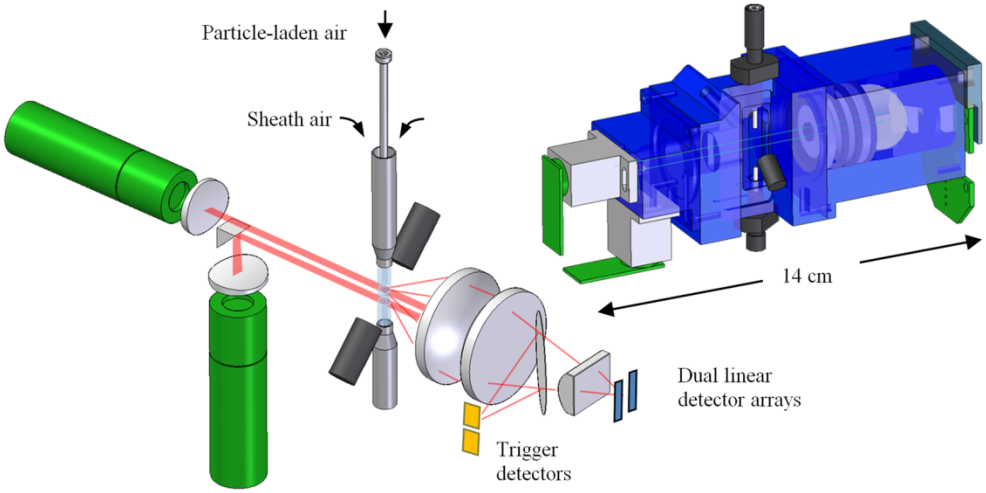

Fig. 9. Schematic diagram of the Dual-beam asbestos detection system. Inset: Cut-away 3D model of the actual Dual-beam system implementation.

In another improvement over the Single-beam system, the Dual-beam system employs a ‘sheathed’ airflow regime in which the particle-laden sample air is surrounded by a relatively wide laminar sheath of particle-free air travelling at the same velocity. This significantly reduces aerodynamic shear forces on the fibers after they leave the inner delivery tube and virtually eliminates air-flow induced alignment changes during their transit between the beams. Any fiber re-alignment during this transit therefore predominantly arises from the influence of the magnetic field alone.

Finally, two photodiode trigger detectors (one for each beam) are used in the Dual-beam system, allowing ‘tracking’ of individual particles through the system even when the particle concentration reaches a point where more than one particle may be in transit between the beams at the same time. As in the Single-beam system, discrimination of fibers from all other particle types is achieved by PTM (Peak-to-Mean) analysis of the CMOS array data when the particle crosses the upper beam. If, from this test, a particle is deemed to be a fiber, then its angles of alignment when passing through the upper and lower beams are evaluated, from which the change in fiber alignment due to the magnetic field is determined.

The performance of the Dual-beam system has been evaluated in an extensive series of controlled laboratory experiments involving aerosols of both asbestos and non-asbestos materials (the latter case included both fibrous and non-fibrous aerosols). During the testing, both the vertical positions of the magnets relative to the two laser beams and the angle of the

#185720 - $15.00 USD Received 20 Feb 2013; revised 9 Apr 2013; accepted 15 Apr 2013; published 2 May 2013

magnets relative to the airflow were varied to ensure the optimal configuration had been achieved. Somewhat unexpectedly, the best performance in terms of differentiating asbestos from non-asbestos fibers was found not when the magnets were at 45° (as predicted by theory) but when they were at 90° to the axis of the airflow.

This is counter-intuitive given that if asbestos fibers enter the magnetic field region with their axes aligned at 90° to the field, they should experience no torque and undergo no re-alignment. However, most of the incoming fibers are *not* perfectly aligned with the airflow but are at some angle to it and so *will* be influenced by the prevailing magnetic field. More importantly, when the magnets are positioned at 90° to the airflow axis, they can be physically much closer together (2.5 mm) without disturbing the airflow between them. This results in a doubling of the prevailing field strength (from 0.26 T to 0.55 T) and a quadrupling of the torque on the fibers (since the torque varies as the square of the field strength [12]).

Figure 10 illustrates the performance of the Dual-beam system (now using magnets at 90°). It shows laboratory data for the *change* in alignment angle (in degrees) of fibers of crocidolite asbestos and gypsum (commonly found in the same buildings as asbestos) during their transit between the upper and lower laser beams. The results show that the probability of a crocidolite asbestos fiber being re-aligned more than 20° is approximately 32 times higher than for a gypsum fiber achieving the same re-alignment by chance.

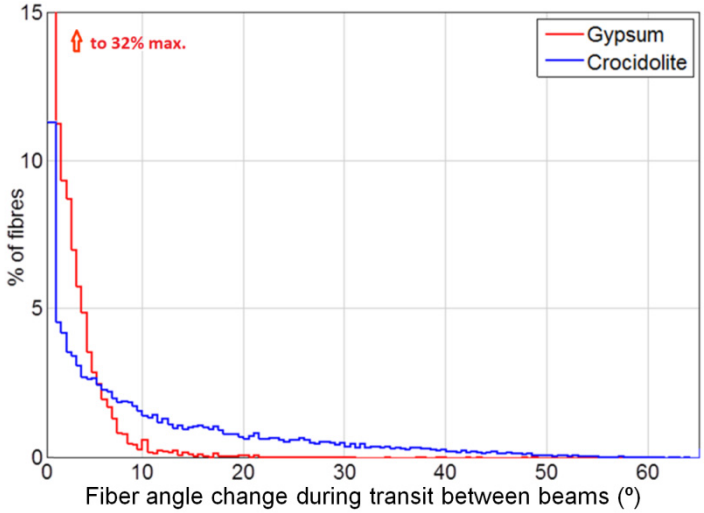

Fig. 10. Absolute change in angle of alignment of crocidolite asbestos fibers and gypsum fibers occurring during fiber transit through the magnetic field region of the Dual-beam system (magnets at 90° to the airflow). Some 2,300 fibers are represented in each population.

4.1 Asbestos detection sensitivity

Given the significant re-alignment in the magnetic field exhibited by asbestos fibers compared to non-asbestos fibers, it is tempting to assume that any fiber detected with a re-alignment of more than 20° would almost certainly be asbestos. However, such a judgment is again ultimately dependent on the relative concentrations of asbestos fibers to non-asbestos fibers present in the aerosol.

We have therefore carried out extensive 2-Sample Test of Proportions [19] statistical analyses of experimental data of the type shown in Fig. 10 to estimate the limits of asbestos detection sensitivity for the Dual-beam system. These analyses suggest that, in the presence of other non-asbestos fibers such as gypsum, glass, mineral wool, etc., crocidolite asbestos fibers can be detected with greater than 99% confidence provided that the crocidolite fibers make up at least ~11% (+/– 2%) of the total population of fibers present in the aerosol. So, for example, a 99% confidence detection of crocidolite asbestos could be achieved where 10,000

#185720 - $15.00 USD Received 20 Feb 2013; revised 9 Apr 2013; accepted 15 Apr 2013; published 2 May 2013

airborne particles were measured, of which 100 were non-asbestos fibers and 12 were crocidolite fibers (the ~9,900 non-fiber particles being rejected at an early stage by the Peak-to-Mean test described in section 3.1). Depending on the concentration of asbestos fibers present, this level of detection could be achieved within a few seconds of measurement. If the ambient aerosol contains only crocidolite asbestos fibers (no other fiber types present), the analysis suggests a positive detection of asbestos could be made with as few as 5 to 10 individual fiber measurements.

Similar statistical analyses of data from chrysotile asbestos, which exhibits a lower paramagnetic anisotropy and therefore a smaller re-alignment in the magnetic field, indicates that for a 99% confidence detection, the chrysotile fibers should make up at least ~45% (+/−5%) of the total fiber population present. If only chrysotile fibers were present, then a 99% confidence detection could be achieved with 30-40 individual fiber measurements.

5. Conclusion and discussion

We have demonstrated that the presence of airborne asbestos fibers can be rapidly detected through an analysis of the spatial light scattering patterns from individual particles carried in a sample airflow through a magnetic field. The analysis serves both to discriminate fiber particles from all other particle types and to subsequently discriminate asbestos from non-asbestos fibers by determining the extent to which the angle of alignment of the fiber is changed under the influence of the magnetic field. Preliminary field testing of portable prototype Dual-beam systems, as described in section 4, has been carried out at various UK locations where asbestos clearance or renovation work was taking place. In each case, the presence or absence of asbestos in the building fabric was known in advance by virtue of earlier statutory asbestos surveys. In each case, the prototype detector systems correctly produced a positive or null response during the clearance or renovation work. Field testing and optimization of the technique is continuing and the authors believe further improvements in asbestos detection sensitivity and particle analysis rate (currently up to 600 particles/s) are achievable.

Acknowledgment

We gratefully acknowledge the support of European Union ‘Research for SMEs’ grant FP7-SME-2008-2 in conducting the above research.

#185720 - $15.00 USD Received 20 Feb 2013; revised 9 Apr 2013; accepted 15 Apr 2013; published 2 May 2013